Numerical Front Propagation Using Kinematical Conservation Laws

K. R. Arun, M. Lukáčová-Medviďová and P. Prasad

1 Introduction

Propagation of a curved nonlinear wavefront or a shock front exhibits a very complex phenomenon of possessing curves of discontinuity, across which the normal to the front and the amplitude distribution on it are discontinuous. Some of these curves of discontinuity are called kinks. A kink is a shock in a corresponding ray coordinate system in which a physically realistic system of conservation laws has been formulated. The conservation form of the system of evolution equations of a curve in two space dimensions was first derived by Morton et al. [8] and this new set of conservation laws is termed as kinematical conservation laws (KCL). The KCL being a pure geometrical result, does not take into consideration any dynamics of the propagating front. This makes the KCL an incomplete system. The closure equation for KCL can be derived by considering the dynamical conditions of the propagating front. Prasad and collaborators have used the KCL along with some closure equations derived on physical considerations to solve several interesting problems, see the review paper [10] and the references therein. The KCL for a surface evolving in three space dimensions, called 3-D KCL, a system of six conservation laws, were first derived by Giles et al. [5]. The 3-D KCL system also contains three divergence-free type stationary constraints, all three together termed as 'geometric solenoidal constraint'. Later, the analysis of the 3-D KCL system, with the closure equation from a weakly

K. R. Arun
Institut für Geometrie und Praktische Mathematik, RWTH Aachen, Templergraben 55, D-52056 Aachen, Germany, e-mail: arun@igpm.rwth-aachen.de

M. Lukáčová-Medviďová
Institut für Mathematik, Johannes Gutenberg-Universität Mainz, Staudingerweg 9, D-55099 Mainz, Germany, e-mail: lukacova@mathematik.uni-mainz.de

P. Prasad
Department of Mathematics, Indian Institute of Science, Bangalore - 560012, India, e-mail: prasad@math.iisc.ernet.in

nonlinear ray theory (WNLRT) [9] was completed by Arun and Prasad [3, 4]. It has been shown in [3] that the resulting system of conservation laws, the so called conservation laws of 3-D WNLRT give rise to a weakly hyperbolic system; in the sense that the system has zero as a repeated eigenvalue with multiplicity five, but the associated eigenspace is only four-dimensional.

Despite the 3-D WNLRT being a weakly hyperbolic system, in [1, 2] we have been able to develop efficient numerical approximations for it using simple, but robust central schemes. It is well known that the solution to the Cauchy problem for a weakly hyperbolic system (with deficiency in dimension of the eigenspace by one) typically contains a mode which grows linearly in time. This mode, the so-called 'Jordan mode', is in the direction of a generalised eigenvector and which can cause severe difficulties in the numerical approximation of such systems. It has been proved in [1] that when the geometric solenoidal constraint is satisfied initially, the solution to the Cauchy problem for linearised 3-D WNLRT at any time does not exhibit the Jordan mode. Motivated by this, a constrained transport technique has been employed to enforce the geometric solenoidal constraint in the numerical solution of 3-D WNLRT, see [1] for more details.

The aim of the present paper is to give a brief overview of the recent results obtained with 3-D WNLRT and to show its efficacy to model propagating wavefronts. The layout of the paper is as follows. In section 2 we introduce the governing equations of 3-D WNLRT. The numerical approximation and the constrained transport strategy are outlined in section 3. In section 4 we present the results of a numerical experiment, showing the efficiency and robustness of the present method. Finally, we close this article with some concluding remarks in section 5.

2 Governing equations

Consider a one parameter family of surfaces in (x_1, x_2, x_3)-space such that it represents the successive positions of a moving surface Ω_t as time varies. Associated with the family, we have a ray velocity $\boldsymbol{\chi}$ at any point (x_1, x_2, x_3) on the surface Ω_t. We consider only the isotropic evolution of Ω_t so that we take $\boldsymbol{\chi}$ to be in the direction of the unit normal $\mathbf{n}$ to Ω_t, i.e. $\boldsymbol{\chi} = m\mathbf{n}$, where m is the normal velocity of propagation of Ω_t. Hence, the evolution of Ω_t is governed by

$$\frac{\mathrm{d}\mathbf{x}}{\mathrm{d}t} = m\mathbf{n}. \tag{1}$$

We introduce a ray coordinate system (ξ_1, ξ_2, t) such that for $t = \text{const}$, we get (ξ_1, ξ_2) as the surface coordinates on Ω_t. Further, $\xi_1 = \text{const}, \xi_2 = \text{const}$ represent the rays, a two parameter family of curves orthogonal to Ω_t. Let $\mathbf{u}$ and $\mathbf{v}$ be respectively the unit tangent vectors to the curves $\xi_2 = \text{const}$ and $\xi_1 = \text{const}$ on Ω_t and let $\mathbf{n}$ be a unit normal to Ω_t. Then we have

$$\mathbf{n} = \frac{\mathbf{u}\times\mathbf{v}}{\|\mathbf{u}\times\mathbf{v}\|}. \tag{2}$$

Let an element of distance along a curve ($\xi_2 = \text{const}, t = \text{const}$) be $g_1 \mathrm{d}\xi_1$. Analogously, denote by $g_2 \mathrm{d}\xi_2$, the element of distance along a curve ($\xi_1 = \text{const}, t = \text{const}$). The element of distance along a ray ($\xi_1 = \text{const}, \xi_2 = \text{const}$) is $m\mathrm{d}t$. Based on geometrical considerations we can derive the 3-D KCL [3, 5],

$$(g_1\mathbf{u})_t - (m\mathbf{n})_{\xi_1} = 0, \tag{3}$$

$$(g_2\mathbf{v})_t - (m\mathbf{n})_{\xi_2} = 0 \tag{4}$$

subject to the condition

$$(g_1\mathbf{u})_{\xi_1} - (g_2\mathbf{v})_{\xi_2} = 0. \tag{5}$$

Note that the constraint (5) is an involution, i.e. if it is satisfied at time $t = 0$, then the equations (3)-(4) imply that it is satisfied for every time. Since each of the components of (5) is a divergence-free type condition, the vector constraint (5) has been designated as geometric solenoidal constraint. The 3-D KCL (3)-(4), being six evolution equations in seven unknowns $u_1, u_2, v_1, v_2, m, g_1$ and g_2, is an underdetermined system. We use the closure equation by considering the energy propagation along the rays of a WNLRT, c.f. [9]. The energy transport equation of WNLRT for a polytropic gas initially at rest and in uniform state can be written in a conservation form [3]

$$\Big((m-1)^2 e^{2(m-1)} g_1 g_2 \sin\chi\Big)_t = 0, \tag{6}$$

where χ is the angle between the vectors $\mathbf{u}$ and $\mathbf{v}$. The system of equations (3)-(4) and (6), hereafter designated as the conservation laws of 3-D WNLRT, is the complete set of equations describing the evolution of the nonlinear wavefront Ω_t.

Remark 1. It has been proved in [4] that the eigenvalues of 3-D WNLRT are $\lambda_1, \lambda_2 (= -\lambda_1), \lambda_3 = \cdots = \lambda_7 = 0$, where λ_1 is given by

$$\lambda_1 = \left\{ \frac{m-1}{2\sin^2\chi} \left(\frac{e_1^2}{g_1^2} - \frac{2e_1e_2}{g_1g_2}\cos\chi + \frac{e_2^2}{g_2^2} \right) \right\}^{1/2}. \tag{7}$$

Here, $(e_1, e_2) \in \mathbb{R}^2$ with $e_1^2 + e_2^2 = 1$. Further, there are only four independent eigenvectors for the eigenvalue zero. Note that λ_1 is real for $m > 1$ and purely imaginary for $m < 1$. Hence, the 3-D WNLRT forms a weakly hyperbolic system when $m > 1$. In this article we consider only the case when $m > 1$.

3 Numerical approximation

In this section we present a numerical approximation of the conservation laws of 3-D WNLRT to study evolution of a weakly nonlinear wavefront Ω_t and formation and propagation of kink curves on it. Note that the system of conservation laws of

3-D WNLRT can be recast in the usual divergence form

$$W_t + F_1(W)_{\xi_1} + F_2(W)_{\xi_2} = 0, \tag{8}$$

where the vector of conserved variables W and the flux-vectors $F_1(W)$ and $F_2(W)$ in the ξ_1- and ξ_2-directions respectively, are given by

$$\begin{aligned} W &= \left(g_1\mathbf{u}, g_2\mathbf{v}, (m-1)^2 e^{2(m-1)} g_1 g_2 \sin\chi\right)^T, \\ F_1(W) &= (m\mathbf{n}, \mathbf{0}, 0)^T, \\ F_2(W) &= (\mathbf{0}, m\mathbf{n}, 0)^T. \end{aligned} \tag{9}$$

In what follows we briefly summarise the central finite volume scheme for (8), first employed in [1].

1. The cell integral averages of W are used in the discretisation of the system of conservation laws (8).
2. A second order TVD Runge-Kutta method [12] is used for time integration. The time-step is chosen to be inversely proportional to the maximum of the nonzero eigenvalue λ_1, c.f. (7), taken over the entire computational domain.
3. A nonlinear iterative solver is employed to recover the values of $\mathbf{u}, \mathbf{v}, g_1, g_2$ and m from the computed values of W.
4. A second order MUSCL reconstruction with a central weighted essentially non-oscillatory (CWENO) limiter [6] is used to reconstruct the variables at the cell interfaces.
5. The Kurganov-Tadmor high resolution flux [7] is used as the numerical flux at a cell interface, for example at a right hand vertical edge

$$\mathscr{F}_{i+\frac{1}{2},j}\left(W^R_{i,j}, W^L_{i+1,j}\right) = \frac{1}{2}\left(F_1\left(W^L_{i+1,j}\right) + F_1\left(W^R_{i,j}\right)\right) - \frac{a_{i+\frac{1}{2},j}}{2}\left(W^L_{i+1,j} - W^R_{i,j}\right), \tag{10}$$

   where $W^{L(R)}_{i,j}$ denote respectively the left and right interpolated states. Here, $a_{i+1/2,j}$ is the maximal wave-speed, which can be computed with the help of the maximum of eigenvalues, c.f. [7]. The numerical flux at a horizontal edge can be computed in an analogous manner.
6. In order that the numerical solution satisfy a discrete version of the geometric solenoidal constraint (5), we use a constrained transport algorithm [11]. We employ three potentials $\mathbb{A}_1, \mathbb{A}_2, \mathbb{A}_3$, corresponding to the three components of the vectors $g_1\mathbf{u}$ and $g_2\mathbf{v}$. Note that the geometric solenoidal constraint (5) implies the conditions

$$g_1 u_k = \mathbb{A}_{k\xi_1},\ g_2 v_k = \mathbb{A}_{k\xi_2},\ k = 1,2,3. \tag{11}$$

   The use of (11) in the 3-D KCL system (3)-(5) immediately yields the evolution equations

$$\mathbb{A}_{kt} - m n_k = 0. \tag{12}$$

We numerically solve (12) to get the updated values of the potentials $\mathbb{A}_k$. The resulting values of $\mathbb{A}_k$ are used to suitably discretise (11) to yield the corrected values of $g_1\mathbf{u}$ and $g_2\mathbf{v}$. It is these updated values, which satisfy a discrete version of (5), see [1] for more details.

At any time t, we approximate the wavefront Ω_t by a discrete set of points $\mathbf{x}_{i,j}(t) := \mathbf{x}(\xi_{1i}, \xi_{2j}, t)$. To get the successive positions of Ω_t, we numerically solve the system of ODEs (1) in the discretised form

$$\frac{\mathrm{d}\mathbf{x}_{i,j}(t)}{\mathrm{d}t} = m_{i,j}(t)\mathbf{n}_{i,j}(t), \tag{13}$$

where $m_{i,j}(t)$ and $\mathbf{n}_{i,j}(t)$ are the corresponding values of m and $\mathbf{n}$ obtained from $\overline{W}_{i,j}(t)$.

In order to start the algorithm, the conserved variable W has to be initialised at each mesh point. Here, some care has to be taken, so that (11) is satisfied by the initial values. Let us assume that the initial wavefront Ω_0 is given a parametric form $\mathbf{x} = \mathbf{x}_0(\xi_1, \xi_2)$, with some appropriate choice of surface coordinates ξ_1 and ξ_2. The initial values for $g_1\mathbf{u}$ and $g_2\mathbf{v}$ and the potentials $\mathbb{A}_1, \mathbb{A}_2, \mathbb{A}_3$ can be chosen to be

$$g_1\mathbf{u}(\xi_1, \xi_2, 0) = \mathbf{x}_{0\xi_1}(\xi_1, \xi_2),\ g_2\mathbf{v}(\xi_1, \xi_2, 0) = \mathbf{x}_{0\xi_2}(\xi_1, \xi_2), \tag{14}$$

$$\mathbb{A}_k(\xi_1, \xi_2, 0) = x_k(\xi_1, \xi_2),\ k = 1, 2, 3. \tag{15}$$

Note that (5) and (11) are satisfied by the above choice of initial values. In the numerical test problem considered here, the normal velocity m on Ω_0 has been assigned a constant value $m_0 = 1.2$. For more details of the numerical scheme and its implementation, we refer the reader to [1].

4 Numerical test problem

We choose initial wavefront Ω_0 in a such a way that it is not axisymmetric. The front Ω_0 has a single smooth dip. The initial shape of the wavefront is given by

$$\Omega_0 : x_3 = \frac{-\kappa}{1 + \frac{x_1^2}{\alpha^2} + \frac{x_2^2}{\beta^2}}, \tag{16}$$

where the parameter values are set to be $\kappa = 1/2, \alpha = 3/2, \beta = 3$. The ray coordinates (ξ_1, ξ_2) are chosen initially as $\xi_1 = x_1$ and $\xi_2 = x_2$. The computational domain $[-20, 20] \times [-20, 20]$ is divided into 401×401 mesh points. The simulations are done up to $t = 2.0, 6.0, 10.0$. We have set non-reflecting boundary conditions for all the variables.

In Figure 1 we plot the initial wavefront Ω_0 and the successive positions of the wavefront Ω_t at times $t = 2.0, 6.0, 10.0$. It can be seen that the wavefront has moved up in the x_3-direction and the dip has spread over a larger area in x_1- and

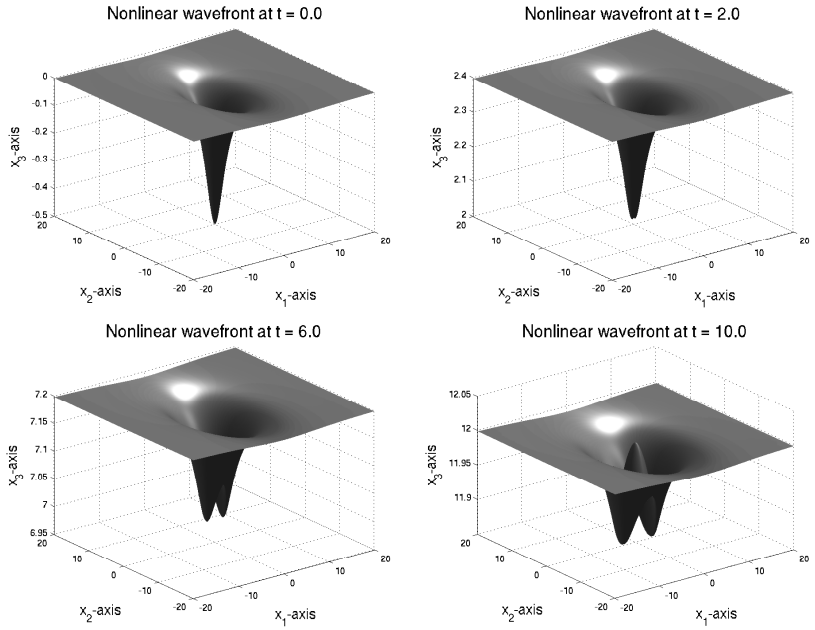

Fig. 1 The successive positions of the nonlinear wavefront Ω_t with an initial smooth dip which is not axisymmetric.

x_2-directions. The lower part of the front moves up leading to a change in shape of the initial front Ω_0. It is very interesting to note that two dips appear in the central part of the wavefront, which are clearly visible at $t = 6.0$ and $t = 10.0$. These two dips are separated by an elevation almost like a wall parallel to the x_2-axis. There is a pair of kink lines, which are also parallel to the x_2-axis and are more clearly seen in Figure 2.

To explain the results of convergence of the rays we also give in Figure 2 the slices of the wavefront in $x_2 = 0$ section and $x_1 = 0$ section from time $t = 0.0$ to $t = 10.0$. Due to the particular choice of the parameters α and β in the initial data (16), the section of the front Ω_0 in $x_2 = 0$ plane has a smaller radius of curvature than that of the section in $x_1 = 0$ plane. This results in a stronger convergence of the rays in $x_2 = 0$ plane compared to those in $x_1 = 0$ plane as evident from Figure 2. In the diagram on the top in Figure 2, we clearly note a pair of kinks at times $t = 3.0$ onwards in the $x_2 = 0$ section. However, there are no kinks in the bottom diagram in Figure 2 in $x_1 = 0$ section.

We give now the plots of the normal velocity m in (ξ_1, ξ_2) plane along ξ_1- and ξ_2-directions in Figure 3. It is observed that m has two shocks in the ξ_1-direction which correspond to the two kinks in the x_1-direction. We have also plotted the numerical values of the divergence of $\mathfrak{B}_1$ at time $t = 10.0$ in Figure 4. It is evident that the geometric solenoidal condition is satisfied with an error of 10^{-15}. The divergences of $\mathfrak{B}_2$ and $\mathfrak{B}_3$ also show the same trend.

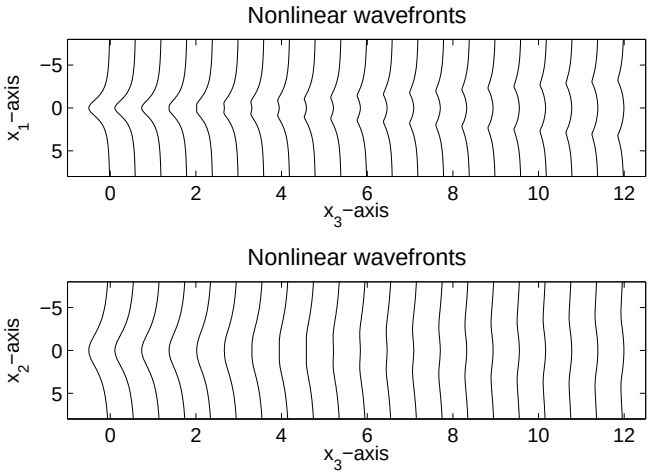

Fig. 2 The sections of the nonlinear wavefront at times $t = 0.0, \ldots, 10.0$ with a time step 0.5. On the top: in $x_2 = 0$ plane. Bottom: in $x_1 = 0$ plane.

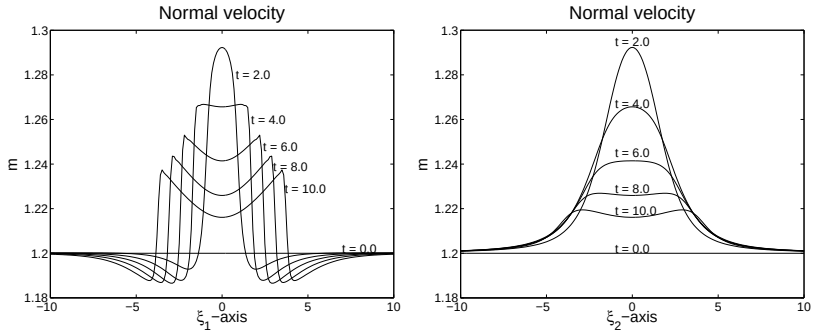

(a) (b)

Fig. 3 The time evolution of the normal velocity m. (a): along ξ_1-direction in the section $\xi_2 = 0$. (b): along ξ_2-direction in the section $\xi_1 = 0$.

5 Concluding remarks

An efficient central finite volume scheme for the weakly hyperbolic system of conservation laws of 3-D WNLRT has been described and tested. Reconstruction is achieved component-wise and a simple central flux is employed in the numerical flux evaluation. Based on our numerical experiment and the ones reported in [1], the solenoidal condition is preserved up to machine accuracy if the present finite volume scheme with a constrained transport technique is used. Moreover, none of the the solution components exhibits any linearly growing Jordan mode.

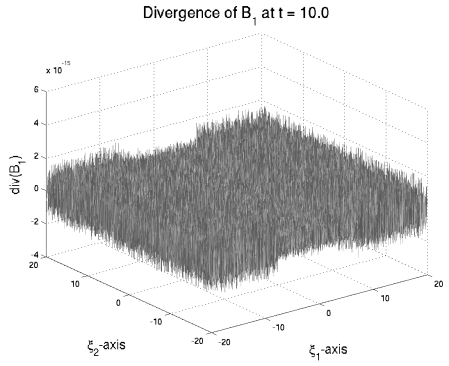

Fig. 4 The divergence of $\mathfrak{B}_1$ at $t = 10.0$. The error is of the order of 10^{-15}.

Acknowledgements K. R. A. wishes to thank the Alexander von Humboldt Foundation for a postdoctoral fellowship. P. P. is supported by the Department of Atomic Energy, Government of India, under Raja-Ramanna Fellowship Scheme.

References

1. Arun, K.R.: A numerical scheme for three-dimensional front propagation and control of Jordan mode. Tech. rep., Department of Mathematics, Indian Institute of Science, Bangalore (2010)
2. Arun, K.R., Lukáčová-Medviďová, M., Prasad, P., Raghurama Rao, S.V.: An application of 3-D kinematical conservation laws: propagation of a three dimensional wavefront. SIAM. J. Appl. Math. **70**, 2604–2626 (2010)
3. Arun, K.R., Prasad, P.: 3-D kinematical conservation laws (KCL): evolution of a surface in $\mathbb{R}^3$-in particular propagation of a nonlinear wavefront. Wave Motion **46**, 293–311 (2009)
4. Arun, K.R., Prasad, P.: Eigenvalues of kinematical conservation laws (KCL) based 3-D weakly nonlinear ray theory (WNLRT). Appl. Math. comput. **217**, 2285–2288 (2010)
5. Giles, M.B., Prasad, P., Ravindran, R.: Conservation forms of equations of three dimensional front propagation. Tech. rep., Department of Mathematics, Indian Institute of Science, Bangalore (1995)
6. Jiang, G.S., Shu, C.W.: Efficient implementation of weighted ENO schemes. J. Comput. Phys. **126**, 202–228 (1996)
7. Kurganov, A., Tadmor, E.: New high-resolution central schemes for nonlinear conservation laws and convection-diffusion equations. J. Comput. Phys. **160**, 241–282 (2000)
8. Morton, K.W., Prasad, P., Ravindran, R.: Conservation forms of nonlinear ray equations. Tech. rep., Department of Mathematics, Indian Institute of Science, Bangalore (1992)
9. Prasad, P.: Nonlinear Hyperbolic Waves in Multi-dimensions. Chapman and Hall/CRC, London (2001)
10. Prasad, P.: Ray theories for hyperbolic waves, kinematical conservation laws (KCL) and applications. Indian J. Pure Appl. Math. **38**, 467–490 (2007)
11. Ryu, D., Miniati, F., Jones, T.W., Frank, A.: A divergence-free upwind code for multidimensional magnetohydrodynamic flow. Astrophys. J. **509**, 244–255 (1998)
12. Shu, C.W.: Total-variation-diminishing time discretizations. SIAM J. Sci. Stat. Comput. **9**, 1073–1084 (1988)